Multi-Stimuli-Responsive Composite Fibers Based on Luminescent Ceramics for UV/Heat Detection and Anti-counterfeiting

Xiuyu Shen[a], Qian Hu[b], Abdolhamid Akbarzadeh[c,d], Chen Shi[a], Zengyuan Pang[a], Mingqiao Ge [a,*]

[a]College Textile Science and engineering, Jiangnan University, Wuxi 214122, China

[b]School of Food Science and Technology, Jiangnan University, Wuxi 214122, China

[c]Department of Bioresource Engineering, McGill University, Montreal, PQ H9X 3V9, Canada

[d]Department of Mechanical Engineering, McGill University, Montreal, QC H3A 0C3, Canada

*Address correspondence to Mingqiao Ge, Email: ge_mingqiao@126.com, Tel: +86-510-85912329, Fax: +86-510-85912329

1. The optimization of $Y_2O_2S:Eu^{3+}$, Mg^{2+}, Ti^{4+}

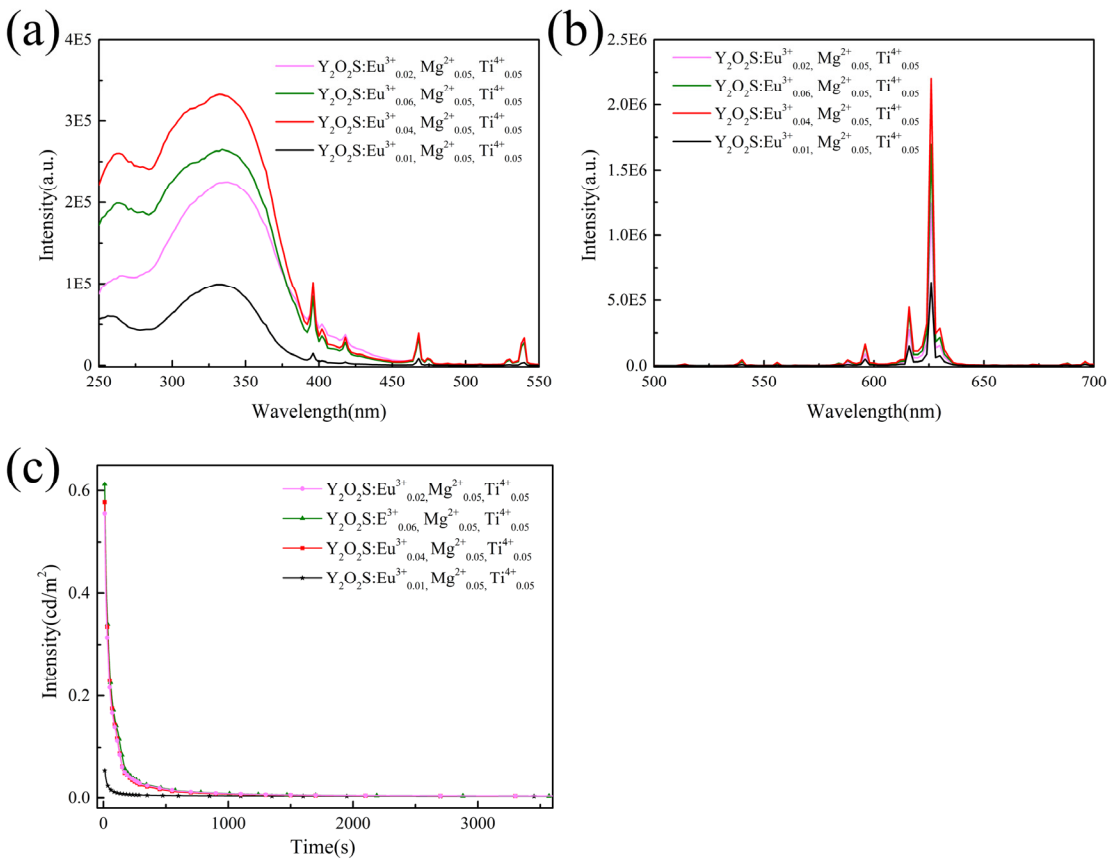

Fig. S1 The (a) excitation spectra, (b) emission spectra and (c) afterglow decay curves of $Y_2O_2S:Eu^{3+}$, Mg^{2+}, Ti^{4+} phosphors with different Eu^{3+} co-doping concentrations.

As shown in Fig S1 (a) and (b), all emission and excitation spectra of $Y_2O_2S:Eu^{3+}$,

Mg^{2+}, Ti^{4+} phosphors with different Eu^{3+} co-doping concentrations present similar pattern. The main excitation peak of samples is in the range of 300-350 nm, which is ascribed to the O^{2-}-Eu^{3+} CTB (charge transfer band) and S^{2-}(3p)-Eu^{3+} CTB respectively, the narrow peaks appear at 396 nm, 468 nm and 540 nm are due to the f-f CT of Eu^{3+}. As shown in Fig 1 (b), the strong red-emission peaks locating at 626nm and 616 nm are due to the transition from $^5D_0$ -$^7F_2$ of Eu^{3+} while some weaker and narrower peaks are ascribed to the ^5D_J (J¼0, 1, 2)-^7F_J (J¼0, 1, 2, 3, 4) of Eu^{3+} ion. It is obvious that the luminescent intensity of $Y_2O_2S:Eu^{3+}_{0.04}$, $Mg^{2+}_{0.05}$, $Ti^{4+}_{0.05}$ is the strongest. Furthermore, the afterglow decay curves of samples under the UV-radiation for 15 min also prove that the persistent luminescent property of $Y_2O_2S:Eu^{3+}_{0.04}$, $Mg^{2+}_{0.05}$, $Ti^{4+}_{0.05}$ is brilliant, although the initial intensity is slightly weaker than $Y_2O_2S:Eu^{3+}_{0.06}$, $Mg^{2+}_{0.05}$, $Ti^{4+}_{0.05}$. Considering the luminescent intensity and the persistent luminescent property, the $Y_2O_2S:Eu^{3+}_{0.04}$, $Mg^{2+}_{0.05}$, $Ti^{4+}_{0.05}$ can be applied in multi-stimuli-responsive fibers.

2. SEM images of 5% and 7% multi-stimuli-responsive fibers

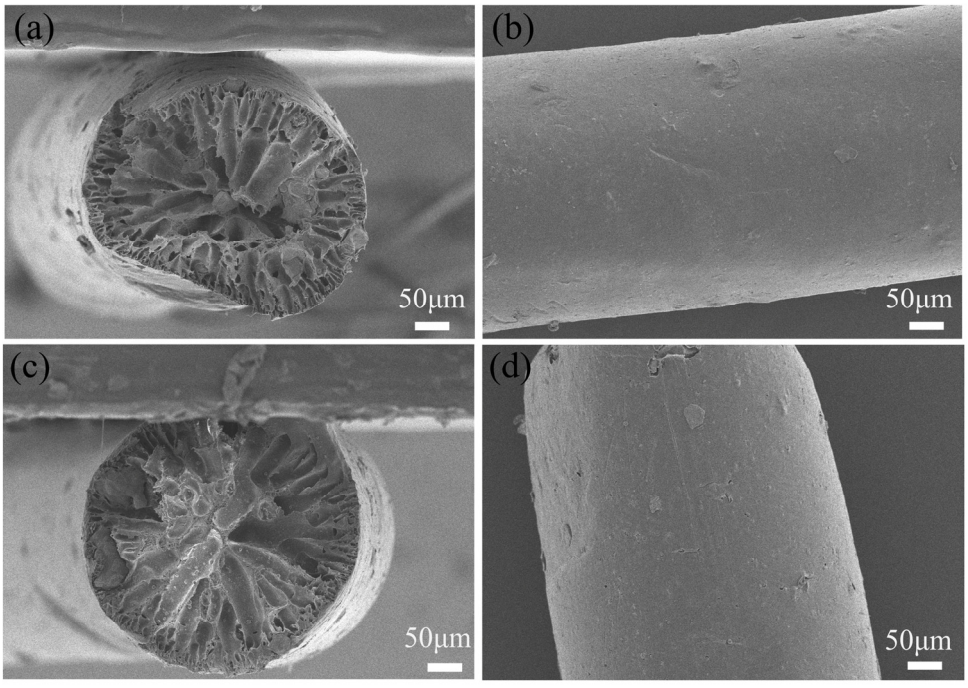

Fig. S2 SEM images of (a) surface, (b) section of 5% multi-stimuli-responsive fibers; (c) surface, (d) section of 7% multi-stimuli-responsive fibers.

3. Sectional elemental distribution maps of 3% multi-stimuli-responsive fibers.

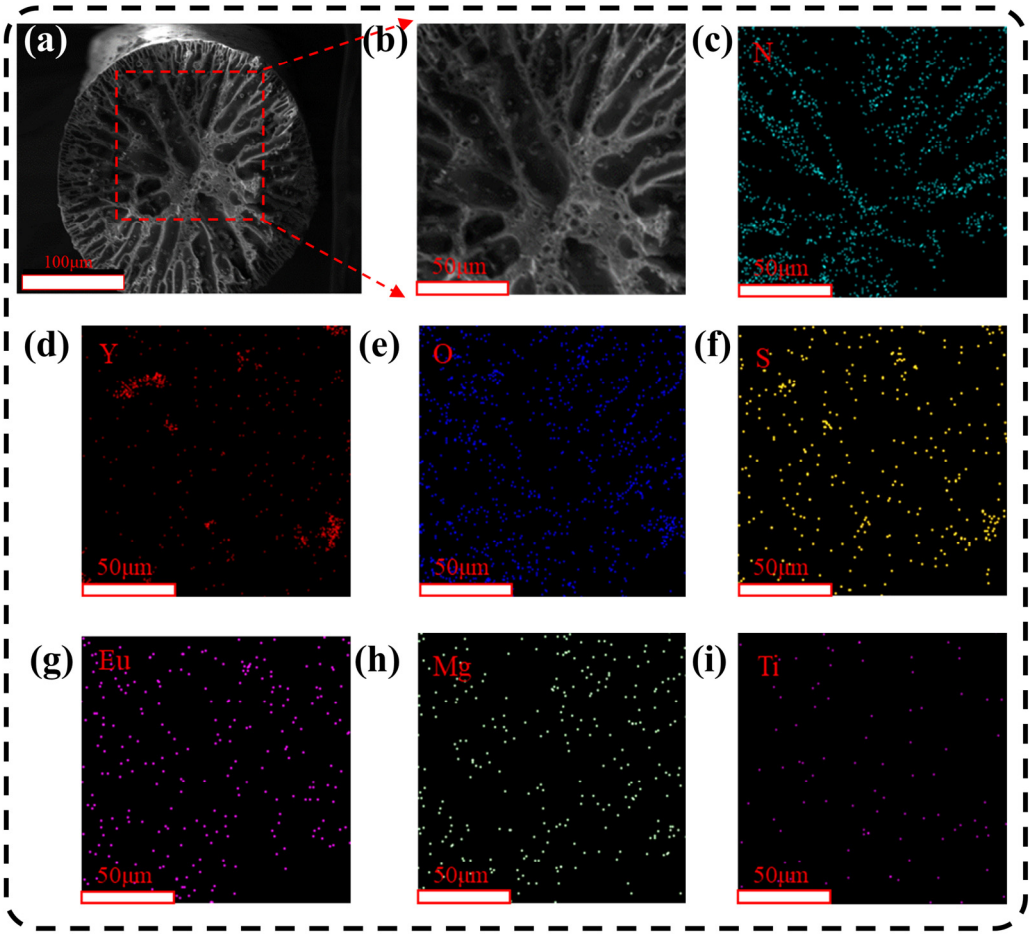

Fig. S3 Sectional elemental distribution maps of 3% multi-stimuli-responsive fibers.

4. PL properties of 3% and 5% multi-stimuli-responsive fibers

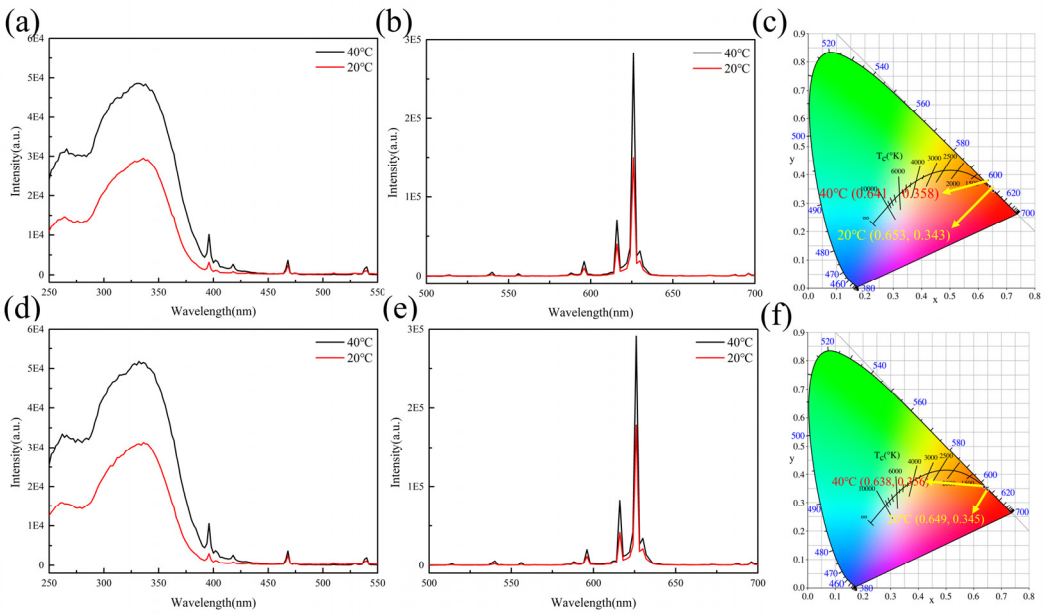

Fig. S4 (a) Excitation spectra (λ_{em}=627nm) and (b) emission spectra (λ_{ex}=330nm) of 5% multi-stimuli-responsive fibers at 20℃ and 40℃; (c) color distribution of 5% multi-stimuli-responsive fibers at different temperature in CIE 1931. (d) Excitation spectra (λ_{em}=627nm) and (e) emission spectra (λ_{ex}=330nm) of 3% multi-stimuli-responsive fibers at 20℃ and 40℃; (f) color distribution of 3% multi-stimuli-responsive fibers at different temperature in CIE 1931.